ELSEVIER

Microelectronic Engineering 30 (1996) 535-538

MICROELECTRONIC ENGINEERING

Micromachined Ultrasonic Air-Transducers (MUTs)

D. Spoliansky[a], I. Ladabaum[b] and B. T. Khuri-Yakub[b]

[a]École Normale Supérieure, 45 rue d'Ulm, 75005 Paris, France

[b]E. L. Ginzton Laboratory, Stanford University, CA94305, United-States

We report work on a new type of ultrasonic transducers, Micromachined Ultrasonic Air-Transducers, which offer a very promising alternative to piezo-electric transducers thanks to micromachining technology. Experiments show that very high frequency signals (11 MHz) can be emitted and detected in air using MUTs. Theoretical explanation for the behavior of MUTs is proposed. It agrees well with experimental results. Optimization will eventually lead to exciting applications of MUTs in medical imaging and non destructive evaluation.

1. INTRODUCTION

An ultrasonic transducer is an electronic device used to emit and to receive acoustic waves. Usual piezo-electric transducers are not very efficient in the conversion between electric and acoustic energy, and their operating frequencies in air are quite low.

MUTs developed in Ginzton Lab rely on micro-machining technology. They are efficient and they can work at very high frequencies in air. Miniaturization and cost effectiveness of their technology will make development of huge arrays of MUTs possible.

We will describe MUTs, explain their static and dynamic behavior and present their process of fabrication. Experimental results will be compared with theoretical predictions.

2. DESCRIPTION OF MUTS

A MUT (fig.1) is an array of silicon nitride membranes vibrating above silicon bulk (fig. 2). The membranes are stretched; their residual stress σ and their radius a determine their resonant frequency.

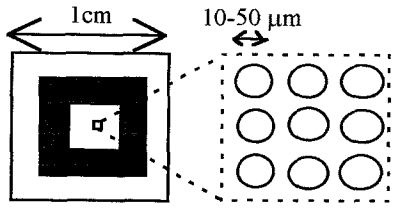

Figure 1. MUT: The device

They can be made to vibrate by applying an alternating voltage between them and the bulk.

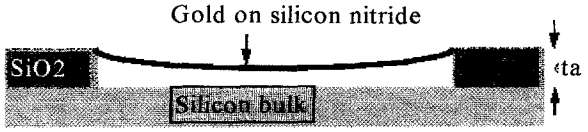

Figure 2. The membrane

The main variables for the study of MUTs are t_m, t_a thickness of the membrane and of the air gap; $x(r)$, vertical displacement of the membrane at radius r; ρ, density of the nitride; Y_0, Young's modulus; ν, Poisson's ratio.

3. STATIC THEORY

We study the electrostatic attraction of a rigidly clamped membrane to underling silicon bulk. When continuous voltage is applied, the attraction tends to pull the membrane towards the bulk, but stress forces resist this movement.

3.1. First order model

The membrane forces are represented by a spring of elastic constant k and the electrostatic attraction by a parallel plate capacitor. Several approximations are made: the electrostatic pressure P_E is taken to be constant and uniform, the stress force to be linearly proportional to the average displacement of the membrane, y, and the expression of the electrostatic pressure is simplified by neglecting the thickness of the membrane. Fringing fields are also neglected.

SSDI 0167-9317(95)00303-7

This model should not be expected to give quantitative results, but it gives an intuitive, analytical approach of the physical problem.

Equilibrium of the membrane in static mode implies the equality of tension and electrostatic forces:

$$\frac{\varepsilon_0 \pi a^2 V^2}{2l^2} = k(t_a - l)$$

Where $l=t_a-y$, and V=continuous voltage. The numerical value of k is approximately 500 N.m^{-1}.

This equation can be converted into a third degree polynom in l, which can be solved. If there are three real roots, of which only the two positive roots have a physical meaning, the membrane is in equilibrium. If there is only one real root, it is negative, so no equilibrium position exists and the membrane collapses on the bulk. The situation in which there is a double positive root corresponds to the collapse point, and occurs when:

$$V_2 = \sqrt{\frac{8}{27}\frac{t_a{}^3 k}{\varepsilon_0 \pi a^2}} \text{ and } l = \frac{2}{3}t_a$$

A second critical point occurs at V_1, when the membrane snaps back, that is when the spring force becomes larger than the electrostatic force. For this analysis, the air-gap has disappeared since the membrane is collapsed, so t_m cannot be neglected.

$$V_1 = \sqrt{\frac{2kt_a t_m{}^2}{\pi a^2 \varepsilon_m}}$$

A plot of displacement as a function of voltage is found on figure 3. Note that the 1/3 collapse is evident, as is the second critical point.

The values used to generate this plot were: t_a=1μm, t_m=0.35μm, a=23μm and k=644N.m^{-1}.

3.2. Improved static model

An improved expression for $P_E(r)$ can be found by considering the thickness of the membrane and of the air-gap at a given point:

$$P_E(r) = \frac{\varepsilon_0 \varepsilon_m^2 V^2}{2\left[t_m \varepsilon_0 + (t_a - x(r))\varepsilon_m\right]^2}$$

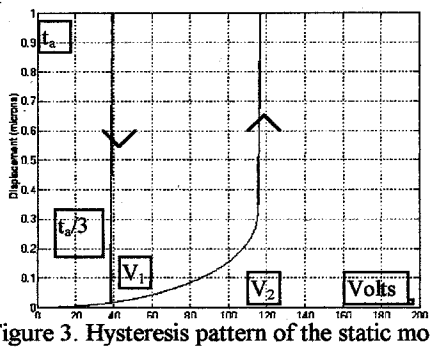

Figure 3. Hysteresis pattern of the static mode

A thin plate with both bending and tension stresses subjected to $P_E(r)$ is governed by (2):

$$\frac{(Y_0 + S\sigma)t_m^3}{12(1-\nu^2)}\nabla^4 x - S\sigma t_m \nabla^2 x - SP_E(r) = 0$$

With boundary conditions : $x(a)=0$ and $dx/dr(a)=0$.

If the membrane is very thin, it has negligible bending stress. The equilibrium equation becomes:

$$\sigma t_m \nabla^2 x + P_E(r) = 0$$

This equation can be solved using an iterative Green's functions method. The Green's function is:

$$G(r,\xi) = \begin{cases} \xi \ln(\xi) \text{ for } 0 < r/a < \xi < 1 \\ \xi \ln(r/a) \text{ for } 0 < \xi < r/a < 1 \end{cases}$$

$$x(r) = \int_0^1 G(r,\xi) P_E(\xi) \frac{a^2}{t_a \sigma t_m} d\xi$$

A collapse is observed with this method when V reaches a certain value. It occurs for displacements larger than 0.4μm, which is in the same range as the 1/3 value predicted by the first order model.

4. DYNAMIC THEORY

During dynamic operation, the voltage applied to the membrane is the superposition of a continuous bias voltage V_{DC} and of an alternating voltage of amplitude V_{AC} and of pulsation ω. This pulsation should match the resonant pulsation of the membrane. $P_E(r)$ then becomes:

$$P_E(r) = \frac{\varepsilon_0 \varepsilon_m^2 (V_{DC}^2 + 2V_{DC}V_{AC}\cos(\omega t) + V_{AC}^2 \cos(\omega t)^2)}{2\left[t_m \varepsilon_0 + (t_a - x(r))\varepsilon_m\right]^2}$$

If $V_{DC} >> V_{AC}$, P_E can be linearized, since the $\cos^2$ term is neglectible. The movement of the membrane is the superposition of the static term we have just calculated and a dynamic term, $u(r)\cos(\omega t)$. The second order equation for $u(r)$ is:

$$\sigma t_m \nabla^2 u + \omega^2 \rho t_m u + P_E(r) = 0$$

If we take the electrostatic pressure as uniform, P, then the solution for a circular membrane is:

$$u(r) = \frac{P}{\omega^2 \rho t_m}\left[\frac{J_0(kr)}{J_0(ka)} - 1\right], \text{ with } k = \omega\sqrt{\frac{\rho}{\sigma}}$$

J_0 being the zeroth order Bessel function. $u(r)$ has a peak displacement when $\omega = 2.405 \times 2\pi\sqrt{\sigma/\rho}/a$.

An equivalent circuit can then lead us to insertion loss and displacement predictions. Very high displacements per volt are predicted.

5. FABRICATION OF MUTS

The transducers are fabricated on highly doped silicon wafers. A 1μm layer of thermal oxide is grown and a 0.35μm layer of silicon nitride is then deposited (residual stress: 320MPa). A 500Å film of gold is evaporated on both sides of the wafer to enable electrical connections. A pattern of 3μm diameter dots with 25, 50 or 100μm period is transferred lithographically to the wafer. The exposed gold and the nitride are then etched, leaving access to the silicon oxide. The wafer is diced to 1 cm square devices and the silicon dioxide is then etched by pure hydrofluoric acid. All these steps are done in a clean room and are summarized on fig. 5.

Depending on the extent of the etch, two configurations can be obtained. If the etch has been performed long enough, the circular etched membranes connect, and only isolated posts of oxide remain. Otherwise, circular membranes are obtained (fig. 4). This configuration is the most frequent, and it corresponds better to the theory developed above. However, there are signs that isolated posts lead to devices with a broader bandwidth.

We fabricated several devices. The 25 μm devices were most efficient at frequencies around 10 MHz, the 50 μm around 5 MHz and the 100 μm around 2 MHz. The silicon dioxide provides the lateral clamping of the silicon nitride membrane. Thus, their period determines the resonant frequency of the device.

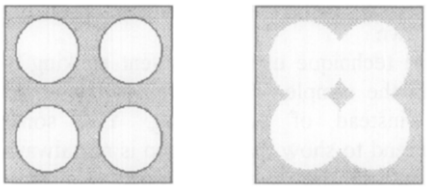

Circular membranes Isolated posts

Figure 4. Membranes and posts

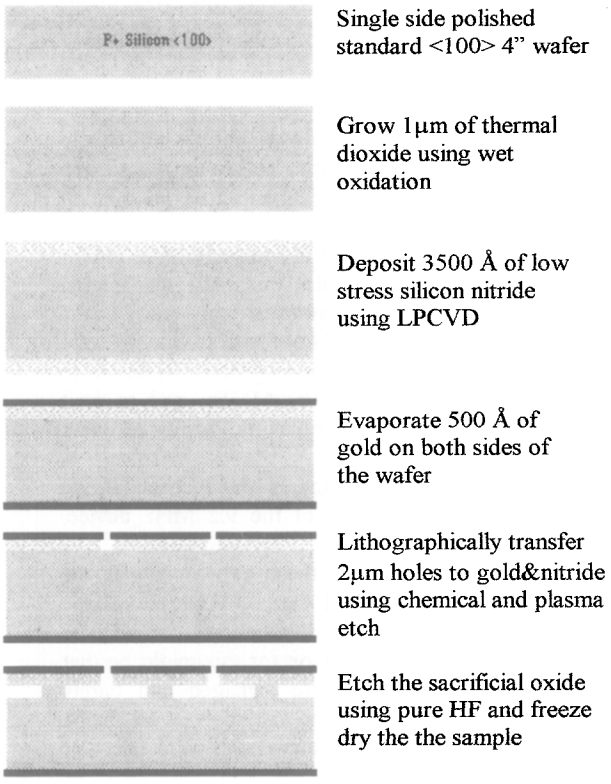

Figure 5. Process of fabrication

The major problem in the fabrication process is membrane sticking. The last processing is a wet etch. As the sample dries, surface tension pulls the nitride

membrane down. Once the nitride and the silicon are in contact, Van der Waals forces hold them together and the device no longer functions. Two different techniques were used to prevent this from occurring. The first technique is a chemical roughening of the silicon surface using KOH. This reduced the surface area that the membrane was exposed to and thus reduces the Van der Waals force holding the membrane down.

The second technique used to prevent sticking is freeze-drying the sample. This results in the liquid sublimating instead of evaporating. Yet, some experiments tend to show that this step is not always necessary. Putting the "wet" transducers in pure alcohol and leaving it evaporate has been shown to prevent sticking for membranes with a relatively small radius.

After the sample has been fabricated, electrical contact must be made to the front and back of the transducer.

6. EXPERIMENTS

The static behavior of the membrane is difficult to check by experimental means. The following section describes dynamic experiments and analyses their fit with theory.

We were most interested in transmission in air for very high frequencies. This was made challenging because attenuation in air varies like the square of the frequency expressed in MHz. The transducers were mounted on platforms with 6 degrees of freedom to ensure proper alignment. The MUTs used to emit and to receive had to have the same resonant frequency.

On figure 6 can be compared the theoretical and the experimental response of the 9.2 MHz device. The fit is very good.

The main problem with these experiments is the weakness of the detected signal. While its shape corresponds to theoretical predictions, its level is lower than expected. A reason for this might be that some of the membranes are damaged and barely work. A new process of fabrication is being developed. It will probably answer this challenge.

7. CONCLUSION

We have described the process of fabrication of a new type of transducer, the MUT. Theoretical explanation of its behavior and experiments were made.

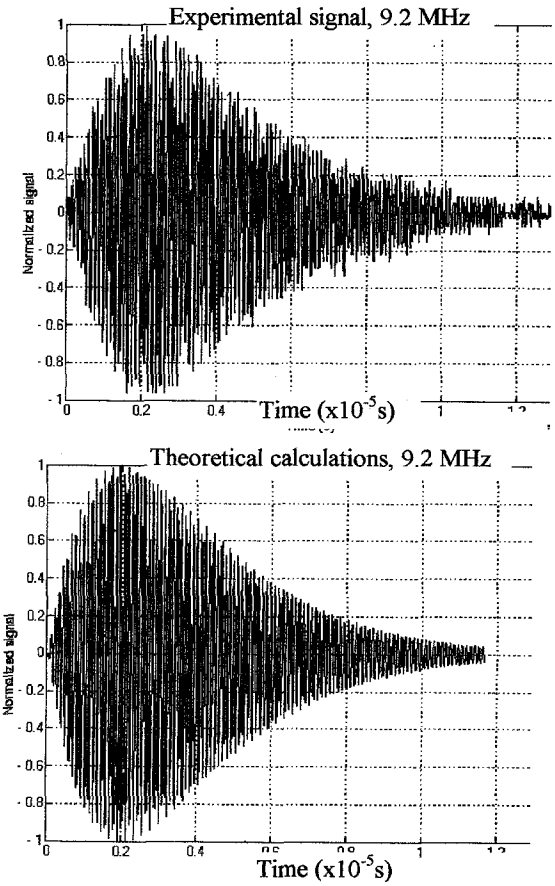

Figure 6. 9.2MHz, experiment and theory

Although some difficulties remain, experiments corroborated theory and showed transmission of ultrasound in air at frequencies above 10 MHz, which had never been achieved before, to our knowledge.

Development of MUT is far from over: a new process of fabrication will give better control of the etching and greater reliability. At that stage of development of the project, the static analysis of the membrane will be essential, and practical applications of MUTs in medical imaging and NDE will be made possible.

REFERENCES

(1) M. I. Haller, *Micromachined Ultrasonic Devices and Materials* Ph. D dissertation, Stanford, 1994

(2) W. P. Mason, *Electromechanical Transducers and Wave Filters,* New-York, Van Nostrand Company, 1942, pp. 163-165, 193-195